HAL
open science

The role of cysteine and sulfide in the interplay between microbial Hg(II) uptake and sulfur metabolism

Sara A. Thomas, Patrice Catty, Jean-Louis F Hazemann, Isabelle Michaud-Soret, Jean-François Gaillard

To cite this version:

Sara A. Thomas, Patrice Catty, Jean-Louis F Hazemann, Isabelle Michaud-Soret, Jean-François Gaillard. The role of cysteine and sulfide in the interplay between microbial Hg(II) uptake and sulfur metabolism. Metallomics, 2019, 11 (7), pp.1219-1229. 10.1039/c9mt00077a . hal-02148519

HAL Id: hal-02148519

https://hal.science/hal-02148519v1

Submitted on 10 Nov 2020

HAL is a multi-disciplinary open access archive for the deposit and dissemination of scientific research documents, whether they are published or not. The documents may come from teaching and research institutions in France or abroad, or from public or private research centers.

L'archive ouverte pluridisciplinaire **HAL**, est destinée au dépôt et à la diffusion de documents scientifiques de niveau recherche, publiés ou non, émanant des établissements d'enseignement et de recherche français ou étrangers, des laboratoires publics ou privés.

METALLOMICS Volume: 11 Issue: 7 Pages: 1219-1229 Published: JUL 1 2019
https://doi.org/10.1039/C9MT00077A

Submitted 03 Apr 2019

Accepted 20 May 2019

First published 22 May 2019

The role of cysteine and sulfide in the interplay between microbial Hg(II) uptake and sulfur metabolism

Sara A. Thomas,[1,2]*+ Patrice Catty,[2] Jean-Louis Hazemann,[3] Isabelle Michaud-Soret,[2]* and Jean-François Gaillard[1]*

[1] Department of Civil and Environmental Engineering, Northwestern University, 2145 Sheridan Road, Evanston, IL 60208

[2] Université Grenoble Alpes, CNRS, CEA, BIG-LCBM, 38000 Grenoble, France

[3] Institut Néel, UPR 2940 CNRS—Université Grenoble Alpes, F-38000 Grenoble, France

*Corresponding authors:

Sara A. Thomas

Email: st18@princeton.edu

Phone: +1 (609)-258-2339

Isabelle Michaud-Soret

Email: isabelle.michaud-soret@cea.fr

Phone: +33 4 38 78 99 40

Jean-François Gaillard

Email: jf-gaillard@northwestern.edu

Phone: +1 (847)-467-1376

+ Present address: Department of Geosciences, Princeton University, Guyot Hall, Princeton, NJ 08544

TOC

Mercury uptake by *E. coli* in the presence of excess cysteine is facilitated by the biodegradation of cysteine to sulfide and the formation of mercury sulfide species. The deletion of a key cysteine desulfhydrase gene (*decR*) limits the uptake of mercury in the presence of excess cysteine.

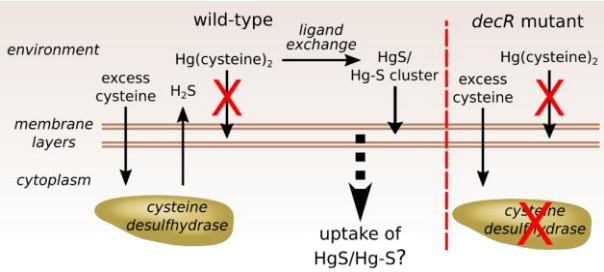

Significance to Metallomics

The present study describes how the cellular sulfur metabolism can influence Hg(II) biouptake by bacteria, potentially leading to the misinterpretation of results if not considered. We demonstrate that the high Hg(II) bioavailability previously observed in the presence of excess cysteine is dependent on the biodegradation of cysteine to sulfide and the formation of cell-associated Hg(II)-sulfide species.

Abstract

Biogenic thiols, such as cysteine, have been used to control the speciation of Hg(II) in bacterial exposure experiments. However, the extracellular biodegradation of excess cysteine leads to the formation of Hg(II)-sulfide species, convoluting the interpretation of Hg(II) uptake results. Herein, we test the hypothesis that Hg(II)-sulfide species formation is a critical step during bacterial Hg(II) uptake in the presence of excess cysteine. An *Escherichia coli* (*E. coli*) wild-type and mutant strain lacking the *decR* gene that regulates cysteine degradation to sulfide were exposed to 50 and 500 nM Hg ± 0.5 to 2 mM cysteine. The *decR* mutant released ~4 times less sulfide from cysteine degradation compared to the wild-type for all tested cysteine concentrations during a 3 hour exposure period. We show with thermodynamic calculations that the predicted concentration of Hg(II)-cysteine species remaining in the exposure medium (as opposed to forming $HgS_{(s)}$) is a good proxy for the measured concentration of dissolved Hg(II) (i.e., not cell-bound). Likewise, the measured cell-bound Hg(II) correlates with thermodynamic calculations for $HgS_{(s)}$ formation in the presence of cysteine. High resolution x-ray absorption near edge structure (HR-XANES) spectra confirm the existence of cell-associated $HgS_{(s)}$ at 500 nM total Hg and suggest the formation of Hg-S clusters at 50 nM total Hg. Our results indicate that a speciation change to Hg(II)-sulfide controls Hg(II) cell-association in the presence of excess cysteine.

Introduction

The bioaccumulation of alkylated mercury (Hg) species poses significant risks to ecosystem and human health. However, the mechanism of bacterial uptake of inorganic Hg(II) species that leads to alkyl-mercury (e.g., methylmercury – MeHg) formation remains unknown.[1] One way to gain insight into the uptake mechanism, which has been extensively investigated in the literature, is to test how the Hg(II) speciation in the exposure medium can affect Hg(II) bioavailability.[2-12] In the environment, Hg(II) is expected to be bound to either thiolate groups of low molecular weight ligands/natural organic matter (NOM) or sulfides due to the high affinity of Hg(II) for reduced sulfur.[13] Among various thiols, exogenous cysteine has been shown to play an important role in regulating Hg(II) uptake, greatly enhancing or inhibiting it depending on the cysteine and Hg(II) concentration.[3-5, 7, 11, 14, 15]

Cysteine is an amino acid that plays a central role in cellular sulfur metabolism.[16, 17] A few of the various metabolic pathways involving cysteine include the biosynthesis of methionine, the formation of iron sulfur (Fe-S) clusters, and the biosynthesis of glutathione.[16, 18-24] The thiolate group of cysteine assists protein folding via the formation of disulfide bonds, exists in the catalytic sites of enzymes, and binds strongly to soft acid metals (e.g., Hg(II), Cd(II), Pb(II), and Ag(I)).[24] However, due to its high reactivity, cysteine is toxic to cells. As a result, cells have complex regulatory systems to maintain strict control of intracellular cysteine concentrations.[17] In response to increased intracellular cysteine concentration, cysteine desulfhydrase and/or desulfidase enzymes are activated to degrade cysteine into hydrogen sulfide, pyruvate, and ammonium.[25-29] Although the biodegradation of biologically important thiols (e.g., cysteine and glutathione) has been well documented,[30-32] past Hg(II) uptake experiments have rarely considered how the Hg(II) speciation in the exposure medium may change over time due to ligand degradation, synthesis, or secretion by the bacteria. The ability of exogenous thiols to degrade into sulfide and the ability of bacteria to produce sulfide endogenously (i.e., not limited to dissimilatory sulfate reduction) is of particular importance for understanding Hg(II) bioavailability due to the evidence that neutrally-charged dissolved and nanoparticulate Hg(II)-sulfide species may be bioavailable to bacteria via passive diffusion.[10, 33, 34]

Previous studies, including our own, have shown, relying on thermodynamic calculations, that the sulfide released from exogenous cysteine degradation can outcompete excess cysteine and bind Hg(II) in the exposure medium.[10, 12, 35, 36] In agreement with these calculations, we have shown using x-ray absorption spectroscopy (XAS) and scanning transmission electron microscopy (STEM) that cell-associated $HgS_{(s)}$ nanoparticles form after the exposure of *Escherichia coli*, *Geobacter sulfurreducens*, and *Bacillus subtilis* to Hg(II) and excess cysteine.[35] Pre-equilibrated Hg(II)-cysteine complexes that are added to cell suspensions will form cell-associated α-$HgS_{(s)}$ or β-$HgS_{(s)}$ at relatively high total added Hg(II) concentrations (500 nM – 5 μM) and short time scales (< 1 hour). At lower added Hg(II) concentrations (50 nM), we also observed the formation of cell-associated Hg(II)-sulfide species from Hg(II)-cysteine complexes. However, the relatively low signal to noise ratio of conventional XAS at these Hg(II) concentrations limited our ability to determine the nature of the Hg(II)-sulfides (e.g., nanoparticulate β-$HgS_{(s)}$ or smaller, β-HgS-like Hg-S clusters). In addition, we were unable to directly relate Hg(II)-sulfide species formation to Hg(II) uptake into the cytoplasm.

The goal of this study is to further investigate Hg(II) bioavailability by testing the hypothesis that when sulfide and cysteine coexist in the exposure medium, Hg(II)-sulfide species, and not Hg(II)-cysteine species, undergo biouptake. Due to the simplicity of modifying the genome, wild-type and mutant strains of *E. coli* lacking single genes involved in sulfide biosynthesis (Δ*decR*, Δ*sufS*, and Δ*iscS*) were chosen for these experiments. We exposed bacterial cells to 50 or 500 nM total Hg(II) that was pre-equilibrated with 0 to 2 mM cysteine so that Hg(II) was introduced to exposure assays as Hg(II)-cysteine complexes with an excess of cysteine. Over a period of 3 hours, we quantified the total cysteine, total sulfide, and total Hg concentration in the exposure medium every hour in order to predict Hg(II) speciation. To identify the cell-associated Hg(II) coordination environment, we probed cell pellets that were exposed to Hg(II) ± cysteine for 3 hours with high energy resolution X-ray absorption near edge structure (HR-XANES) spectroscopy.

Materials and methods

Bacterial strains

Keio collection strains of *E. coli* single-gene deletion mutant JW0437 (Δ*decR*, formerly known as Δ*ybaO*) as well as wild-type *E. coli* K-12 (BW25113) were obtained from the *E. coli* Genetic Stock Center.[37] The cysteine desulfurase mutants (Δ*iscS* and Δ*sufS*) were obtained from the BioCat team in the Chemistry and Biology of Metals Laboratory (Grenoble, France) and are described in detail in Ranquet et al.[38] The strains were regenerated from sterile filter disks or frozen glycerol stock (stored at -80 ºC) onto LB agar (with 50 mg/L kanamycin for mutants) at 37 ºC for 24 hours. The strains were stored on LB agar plates at 4 ºC for no longer than 4 weeks.

Growth media and cell harvesting

A single colony of *E. coli* from a refrigerated LB agar plate was inoculated into ~3 mL of LB broth in a sterile, 12 mL polypropylene tube and incubated aerobically at 37 ºC with medium shaking for ~6 hours. Subsequently, 20 – 100 µL of the cell suspension was inoculated into 50 – 100 mL of minimal salts medium (MSM; Table S1) in sterile, foil-topped 125 mL or 250 mL Erlenmeyer flasks and shaken at 37 ºC overnight. Cells were harvested in MSM during exponential growth phase (OD_{600} = 0.2). Cells were washed twice with minimal complexing medium (MCM) – the exposure medium for Hg(II) biouptake assays – and resuspended to a density of 2×10^8 cells/mL, which is equivalent to an OD_{600} of 0.2. MCM is buffered to pH = 7.1 with 20 mM MOPS and contains 1 mM Na-β-glycerophosphate, 0.41 mM $MgSO_4$, 12 mM NH_4NO_3, 0.76 mM isoleucine, 0.76 mM leucine, 3 nM thiamine, 10 mM glucose, and 9.1 mM NaOH.[8] All mutant strains of *E. coli* were grown in the presence of 50 mg/L kanamycin.

Hg(II) and cysteine exposure assays

A 10 mM $Hg(NO_3)_2$ stock solution in 1% HNO_3 (trace metal grade; TMG) was used for all exposure assays and stored at 4 ºC. A 100 mM cysteine stock solution was prepared in deionized water (18 MΩ) immediately before use. Hg(II) and cysteine were pre-equilibrated for 1 hour in deionized water (18 MΩ) at 10 times the final desired concentrations (fixed molar ratios of 1:2,000, 1:10,000, 1:20,000, or 1:40,000

Hg:Cys) prior to being added to cell suspensions. Hg(II) and cysteine exposure assays were aerobic and conducted in 15 mL borosilicate glass vials or 125 mL Erlenmeyer flasks with 7 mL and 50 mL total volume, respectively. The assays were conducted under dark conditions at 37 ^{o}C and initiated with the addition of Hg(II) solution (± cysteine) to the cell suspension in MCM so that the Hg(II) solution (± cysteine) was diluted by a factor of 10. The pH was measured before and after exposure to Hg(II) ± cysteine in MCM and did not significantly vary from the initial pH of 7.1.

Hg(II)-cell sorption measurements

After cell suspensions mixed with Hg(II) and cysteine for 0, 1, 2, and 3 hours (7 mL total volume), ~700 µL aliquots were collected at each time point for the determination of (1) total recoverable Hg (dissolved + cell-bound) and (2) dissolved Hg (after filtration on a 0.2 µm nylon filter, VWR International). As we documented earlier, the nylon filters do not bind a significant amount of Hg.[36] The samples at 0 hours were collected as soon as possible after Hg addition to cell suspensions, and thus, cells were exposed to Hg(II) for up to 1 minute of mixing. The cell-bound Hg was calculated as the difference between the total recoverable Hg and the dissolved Hg. Samples for determining dissolved and total recoverable Hg were preserved in ~1% HCl (TMG) until the measurement of total Hg with a Direct Mercury Analyzer (DMA-80, Milestone).

Sulfide and cysteine detection in the exposure medium

After mixing cells with cysteine for 0, 1, 2, and 3 hours (7 mL total volume), a 1 mL aliquot was centrifuged (15,000 g for 5 min) for the determination of acid labile sulfide in the supernatant by a method adapted from Cline[39, 40] as well as cysteine and cystine (oxidized cysteine) by a method adapted from Gaitonde.[41] Both the Cline and Gaitonde methods are colorimetric and specific to sulfide and cysteine, respectively. Detailed methods are reported in our previous publication.[36] The detection limit for sulfide and cysteine was 2 µM and 5 µM, respectively.

Bacterial samples for HR-XANES measurements

After a 3 hour exposure of cells to Hg(II) ± cysteine (50 mL total volume), the cells were washed 2 times by centrifugation (8,000 g for 5 min) with an equivalent volume of 0.1 M $NaClO_4$.[42] During the washing steps, the cell suspension was resuspended in smaller volumes in succession until cells were in a 1 mL final suspension of 0.1 M $NaClO_4$. The 1 mL of suspension was added to a 1.5 mL centrifuge tube containing a 0.2 µm cellulose acetate centrifugal filter (~8 mm diameter cut with a hole punch). The tube was centrifuged briefly for 2 minutes at ~3,000 g so that the cells were collected on the filter and the medium passed through the filter. The filter paper containing pelleted cells was subsequently sandwiched between 2 pieces of Kapton tape and immediately plunged in liquid nitrogen. The samples were stored at -80 ^{o}C for no more than 1 week and remained frozen throughout analysis.

HR-XANES experimental setup and analysis.

The HR-XANES experiments were performed at the European Synchrotron Radiation Facility (ESRF) at beamlines BM30B FAME and BM16 FAME-UHD. All Hg standards and samples were measured in high energy resolution fluorescence detection (HERFD) mode with 5 spherically bent Si(111) crystal analyzers (bending radius = 1 m, crystal diameter = 0.1 m). The Hg $L_{\alpha 1}$ fluorescence line (apparent core-hole lifetime broadening of 2.12 eV)[43] was selected using the 555 reflection, and the diffracted fluorescence was measured with a silicon drift detector (SDD, Vortex EX-90). The monochromator was calibrated with a Se reference foil (K-edge = 12,658 eV), and a $HgCl_2$ powder was scanned at the start of each experiment to maintain relative energy calibration. Hg powder standards were finely ground, diluted to ~0.5 wt% with boron nitride, pressed into ~5 mm diameter pellets, and loaded onto a copper sample holder. Liquid Hg reference standards were pipetted into a copper sample holder sealed on two ends with Kapton tape and immediately plunged into LN_2 to minimize contact of the liquid with the copper as well as to prevent the formation of ice during freezing. Frozen bacterial samples were fixed onto copper sample holders with grease and quickly plunged into liquid nitrogen to prevent the sample from thawing. All liquid Hg references and bacterial samples containing Hg were measured at 10 – 15 K. Powdered Hg references (α-$HgS_{(s)}$ and β-$HgS_{(s)}$) were measured at 10 – 15 K and room temperature for comparison.

Data normalization and linear combination fits of the XANES to determine the Hg speciation in bacterial samples were performed with Athena.[44] Details on the preparation of Hg reference standards for HR-XANES is provided in the SI (page S2).

Sample preparation and imaging with TEM

After mixing cells with Hg(II) ± cysteine for 3 hours, a 1 – 2 mL aliquot was collected and washed 4 times with 0.1 M $NaClO_4$ by centrifugation (8000 g for 3 min) in a 1.5 – 2 mL microfuge tube to remove Hg not associated with cells. After the final wash, the cells were resuspended in a solution of 200 µL filtered Milli-Q water (0.2 µm filter, VWR International). One drop (< 5 µL) was immediately placed on a 200 mesh carbon-coated copper grid and allowed to air dry for ~10 minutes. TEM micrographs and selected area electron diffraction (SAED) patterns were collected at room temperature with a Hitachi H-8100 transmission electron microscope using an accelerating voltage of 200 kV.

Thermodynamic calculations

The speciation calculations for Hg(II) were performed with the program ChemEQL.[45] The equilibrium constants used in the calculations are reported in Table S2.

Results and Discussion

Sulfide production from cysteine degradation

The transcription factor DecR (formerly known as YbaO) activates the *yhaOM* operon, where the *yhaO* gene is predicted to be responsible for cysteine import and the *yhaM* gene appears to have cysteine desulfhydrase (also known as desulfidase) activity.[28] *yha*M is cysteine-inducible and has been shown to have the most significant role in cysteine detoxification in *E. coli* among the numerous other reported enzymes (e.g., TnaA, CysK, CysM, MalY, and MetC).[46] The deletion of the *decR* gene was previously shown to strongly limit the desulfhydrase activity in *E. coli*.[28] We exposed a wild-type and *decR* deletion mutant strain of *E. coli* to cysteine concentrations ranging from 0 to 2 mM and measured the total acid

labile sulfide concentration in the exposure medium every hour for 3 hours (Figure 1) by the Cline method.[39]

All added cysteine concentrations tested lead to essentially the same sulfide concentration in the exposure medium at each time point for both the wild-type and *decR* mutant, indicating that cysteine degradation to sulfide reaches a threshold for both strains at 0.5 mM added cysteine and above. Notably, the sulfide concentration in the exposure medium reaches a maximum of ~40 µM (2 hours) for the wild-type strain but only ~10 µM (1 – 2 hours) for the *decR* mutant. After just 1 hour of exposure, the measured sulfide concentration in the exposure medium for all added cysteine concentrations is ~20 µM and 5 -10 µM for the wild-type and *decR* mutant, respectively. Although the *decR* mutant is still able to degrade cysteine and release sulfide into the exposure medium, the loss of cysteine desulfhydrase activity results in a significant decrease in the concentration of total sulfide in the exposure medium.

The concentrations of reduced and total cysteine (i.e., reduced + oxidized) in the exposure medium have also been quantified under the same conditions as the sulfide measurements (Figure 2) by the Gaitonde method, which is cysteine-specific and not affected by similar thiols (e.g., glutathione and homocysteine).[41] A Tukey's honest significant differences test was performed on the wild-type and *decR* mutant datasets for each added cysteine concentration (i.e., 0.5, 1, and 2 mM) to determine the statistical significance ($p < 0.05$) between the measurements. At t = 0 hours, the concentration of reduced cysteine is less than the total cysteine due to the known oxidation of cysteine in the exposure medium.[35, 36] Thus, all assays begin with reduced cysteine concentrations that are ~70 to 90% of the total added cysteine, with cystine accounting for the remainder. With increased incubation time, the cysteine concentration in all assays decreases, mainly due to cysteine biouptake/biodegradation and not oxidation because the total cysteine concentration (reduced + oxidized) also decreases by nearly the same amount. The most notable decrease in cysteine concentration is observed in the wild-type cells exposed to 0.5 mM cysteine, where the initial reduced cysteine concentration drops from ~0.35 mM to ~0.2 mM after 2 hours of exposure. The decrease in the concentration of cysteine is not as drastic for the *decR* mutant under the same

conditions because it has lost some ability to import and degrade cysteine. For the higher total added cysteine concentrations of 1 and 2 mM, the cysteine concentration in the exposure medium decreases over time, but the differences between the wild-type and *decR* mutant are not statistically significant.

Hg sorption measurements and thermodynamic calculations

The concentration of dissolved and cell-bound Hg was quantified in wild-type and *decR* mutant assays as a function of incubation time, added cysteine, and added Hg (Figure 3). For many measurements, the sums of the dissolved and cell-bound concentrations do not add to the total added Hg, which we observed in our previous studies on *E. coli*.[35, 36] We interpreted this as a result of Hg(II) reduction to Hg(0), potentially from outer membrane cytochromes,[47] and loss from volatilization. When the wild-type and *decR* mutant were exposed to either 50 nM or 500 nM Hg without cysteine, the cell-bound Hg is between 40 to 70% of the total added Hg after 1 hour of exposure and does not change significantly after 3 hours (Figure 3A,E,G, and K). The dissolved Hg for these conditions remains between 0 and 5% of the total added Hg after 1 hour of exposure, demonstrating efficient Hg(II) sorption by cells in the absence of added cysteine.

To understand whether conditions favored Hg(II)-sulfide or Hg(II)-cysteine species formation for the experiments involving cysteine exposure in Figure 3, we calculated the Hg(II) speciation in the exposure medium at each time point (Figure 4). Specifically, we present the sum of the concentrations of the Hg(II)-cysteine species as well as $HgS_{(s)}$ (dissolved Hg(II)-sulfide species were negligible) as a fraction of the total added Hg. Our thermodynamic calculations incorporated the total sulfide, cysteine (reduced), and total recoverable Hg concentration measured in the exposure medium (e.g., information from Figures 1, 2, and 3), which we also summarize in Table S3 for reference. We did not test the exposure medium for thiols secreted by the cells (e.g., glutathione). However, it is not likely that secreted thiols would reach a concentration in the exposure medium that could influence Hg speciation in the presence of 0.5 – 2 mM added cysteine. The measured total recoverable Hg was used in these calculations so that the results reflect whether the conditions would favor $HgS_{(s)}$ or Hg(II)-cysteine formation prior to

Hg(II) sorption to cells. Our predictions for $HgS_{(s)}$ formation in the presence of excess cysteine generally agree with the measured fraction of cell-bound Hg. For example, we predict a significant amount of $HgS_{(s)}$ formation when the wild-type strain is exposed to 50 nM Hg(II) and 0.5 or 1 mM cysteine as well as 500 nM Hg(II) and 1 mM cysteine (Figure 4A,B,D), and we concurrently observe a significant amount of cell-bound Hg (Figure 3B,C,F). In addition, when the *decR* mutant strain is exposed to 50 nM Hg and 0.5 mM cysteine as well as 500 nM Hg and 1 mM cysteine, we predict a majority of $HgS_{(s)}$ formation (Figure 4E,H) and observe a majority of cell-bound Hg(II) (Figure 3H,L). The one exception is the 1 hour time point for the *decR* mutant exposed to 50 nM Hg and 0.5 mM cysteine where $HgS_{(s)}$ is predicted to be ~50% of the total added Hg (Figure 4E), but the measured fraction of cell-bound Hg(II) is <10% of the total added Hg (Figure 3H). When the majority of Hg(II) is predicted to remain bound to cysteine in the exposure medium (i.e., Figure 4C,F,G), we see little cell-bound Hg(II) and mostly dissolved Hg(II) (Figure 3D,I,J). Thus, there appears to be a link between dissolved Hg(II) and Hg(II)-cysteine complexes outside the cell due to insufficient sulfide production to shift the equilibrium to $HgS_{(s)}$ formation in the presence of excess cysteine.

ATP measurements

In healthy cells, ATP concentrations are highly regulated and thus can be used as an indicator of biological stress.[48] We assessed the potential toxic effects of cysteine exposure to the wild-type and *decR* mutant strains by quantification of cellular ATP (Figure S1). The wild-type strain does not experience any significant decrease in cellular ATP upon exposure to 50 nM Hg ± 1 and 2 mM cysteine or 500 nM Hg ± 1 mM cysteine for 3 hours (Figure S1A) compared to the cellular ATP concentration prior to exposure. However, the *decR* mutant does observe a statistically significant 10 – 20% drop ($p < 0.05$) in cellular ATP when exposed to 50 nM Hg + 1 and 2 mM cysteine as well as 500 nM Hg ± 1 mM cysteine (Figure S1B). This decrease does not indicate a major change in cellular metabolism. Exposure of the *decR* mutant to 1 and 2 mM cysteine without Hg causes the same observed decrease in ATP concentration (data not shown), suggesting that the effect is due to cysteine alone. Interestingly, the greatest drop in cellular

ATP is observed when the *decR* mutant is exposed to 500 nM Hg without cysteine, where ATP levels are $1.4 \pm 0.2 \times 10^{-18}$ mol per cell after a 3 hour exposure (a 36% drop).

Cell-associated Hg(II) coordination environments

While the detection limit restricts our ability to directly measure Hg(II) speciation in the exposure medium, we are however able to directly probe the Hg(II) coordination environment in bacterial cells by XAS for the conditions in this study. Specifically, Hg L_{III}-edge HR-XANES data were collected to drastically improve the resolution of spectral features compared to conventional XANES.[43] The use of crystal analyzers removes most, if not all, of the contribution of the background fluorescence photons, and therefore, one can investigate the Hg(II) coordination environment in dilute systems (< 1 ppm).[49-52]

To corroborate the predictions for $HgS_{(s)}$ formation and subsequent cell-association, we analyzed select samples from Figures 3 and 4 by HR-XANES: wild-type and *decR* mutant exposed to 500 nM Hg(II) ± 1 mM cysteine and 50 nM Hg(II) ± 1 mM cysteine for 3 hours (Figure 5). Hg L_{III}-edge HR-XANES reference spectra are presented in Figure S2. The references of Hg(II) bound to two sulfur atoms (i.e., α-$HgS_{(s)}$ and Hg(cysteine)$_2$) contain a sharp, in-edge peak that represents a $2p_{3/2} \rightarrow 6s/5d$ electronic transition.[51] This peak is absent in reference spectra of Hg bound to four sulfur atoms (i.e., β-$HgS_{(s)}$ and Hg(cysteine)$_4$). Because the Hg(cysteine)$_2$ species at pH = 11.6 also has two coordinating nitrogen atoms at 2.51 Å,[50] the in-edge peak is not as sharp as those with solely 2 sulfur atoms in the coordination sphere. In addition, the HR-XANES spectra of the two bulk $HgS_{(s)}$ minerals – α-$HgS_{(s)}$ and β-$HgS_{(s)}$ – contain defined peaks above the absorption edge that are lacking in the Hg(II)-thiol references. Thus, determining the Hg(II)-sulfur coordination number and nature of the coordinating ligands (e.g., thiol or sulfide) can be achieved with just the HR-XANES. Linear combination fit results, considering the Hg references described above, are shown in red in Figures 5A,B,E,F,G. Some of the spectra are lacking best-fit curves due to the absence of appropriate reference standards to explain the Hg(II) coordination environment (Figure 5C,D,H). The HR-XANES of *E. coli* wild-type samples exposed to 500 nM Hg(II) ± 1 mM cysteine are best fit with β-$HgS_{(s)}$ and Hg(cysteine)$_2$ references (Figures 5A,B), confirming our previous

results from conventional XAS techniques for exponentially-growing *E. coli*.[35, 36] Because we observe cell-associated β-$HgS_{(s)}$ when 500 nM Hg is added without cysteine, it is clear that an endogenous sulfide source beyond cysteine desulfhydrase exists and binds Hg(II). The aqueous $Hg(cysteine)_2$ at pH = 3 standard was a better fit to the spectra than the $Hg(cysteine)_2$ at pH = 11.6, suggesting that Hg(II) exists as RS-Hg-SR with insignificant Hg-N bonding. This coordination environment is expected when Hg(II) is bound to 2 cysteine residues in a protein, as is the case when Hg(II) is bound to MerP,[53] because the amine groups do not coordinate Hg(II). The spectrum of wild-type *E. coli* exposed to 500 nM Hg(II) and 1 mM cysteine highly resembles the β-$HgS_{(s)}$ reference standard collected at room temperature. Manceau et al. found that well-crystallized β-$HgS_{(s)}$ HR-XANES spectra measured at room temperature resemble those of nanoparticulate β-$HgS_{(s)}$ measured at liquid helium temperature (~10 K),[51] suggesting that the β-$HgS_{(s)}$ associated with *E. coli* is nanoparticulate. We confirmed the presence of cell-associated $HgS_{(s)}$ nanoparticles (~100 nm diameter) with transmission electron microscopy (TEM) (Figure S4). The absence of diffraction spots in the selected area electron diffraction (SAED) pattern implies that the β-$HgS_{(s)}$ nanoparticles are amorphous (Figure S4C).[35]

Surprisingly, the *decR* mutant contained more β-$HgS_{(s)}$ when exposed to 500 nM Hg(II) compared to the wild-type (75.6% vs. 58.7%; Figure 5A and 5E). Thus, the removal of one pathway for cysteine degradation to sulfide in the cell actually increased the presence of cell-associated β-$HgS_{(s)}$. This increase in β-$HgS_{(s)}$ formation could be a result of increased expression of other genes with cysteine desulfhydrase ability to compensate for the loss of *decR*. Additionally, the Hg(II) species associated with the *decR* mutant exposed to 500 nM Hg and 1 mM cysteine was primarily α-$HgS_{(s)}$, unlike the wild-type where cell-associated Hg(II) was primarily β-$HgS_{(s)}$. We also detected the presence and phase of α-$HgS_{(s)}$ with TEM and SAED (Figure S5 and Table S4). We previously observed the formation of *E. coli*-associated α-$HgS_{(s)}$ exclusively when cysteine was present with Hg(II) and sulfide in the exposure medium, suggesting that cysteine plays a role in determining the phase of $HgS_{(s)}$.[35] We predicted that the ratio of total sulfide to total Hg(II) determines the phase of $HgS_{(s)}$ in the presence of cysteine. In this study, we confirmed this

prediction because cell-associated α-$HgS_{(s)}$ forms at a total sulfide to total recoverable Hg(II) ratio of 15 and β-$HgS_{(s)}$ forms at a ratio of 67, similar to the ratios that determined whether α-$HgS_{(s)}$ (10) or β-$HgS_{(s)}$ (100) formed in our previous study.[35] Because our TEM results also reveal that the $HgS_{(s)}$ particle diameters are ≤ 100 nm, we confirm that the cell-bound Hg(II) measurements from Figures 3F,L are actually depicting cell-associated Hg(II) and not just $HgS_{(s)}$ particles in solution that are trapped by the 200 nm pore size filter. $HgS_{(s)}$ nanoparticles are lipophilic, as determined by octanol-water partitioning experiments,[54] which supports our finding that $HgS_{(s)}$ would prefer to attach to lipophilic cell surfaces.

Linear combination fits to the HR-XANES spectra of wild-type and *decR* mutant *E. coli* exposed to 50 nM total Hg(II) ± 1 mM cysteine do not fit well with the references in this study. However, a fairly good fit is achieved with the *decR* mutant exposed to 50 nM Hg(II) considering 49.7% β-$HgS_{(s)}$ and 50.3% $Hg(cysteine)_2$ species at pH = 11.6 (Figure 4G). The wild-type and mutant strains that were exposed to 50 nM Hg(II) and 1 mM cysteine resemble the bulk β-$HgS_{(s)}$ reference standard measured at room temperature, with slight differences. What is clear is that a sharp in-edge peak is absent, indicating that there is not a significant amount of Hg that is linearly coordinated to 2 sulfur atoms. We provide the spectrum of an aqueous $Hg(cysteine)_2$ reference at pH = 5 (Figure S3D) made at similar concentration (wt/wt) as the bacterial samples with the lowest Hg content to show that the in-edge peak characteristic of 2-coordinate Hg-S would be clearly visible. Because the HR-XANES also do not resemble those of $Hg(SR)_2$, $Hg(SR)_3$,[55] or $Hg(SR)_4$ and are lacking features above the edge characteristic of $HgS_{(s)}$ particles,[51] it is likely that Hg(II) exists as Hg-S clusters (i.e., analogous to Fe-S clusters or β-Hg_xS_y less than 1 nm in diameter[56]) with a coordination number of 4.

We also probed single gene deletion mutants of *E. coli* lacking cysteine desulfurase genes (i.e., *iscS* and *sufS*) with HR-XANES to explore the potential biogenic sulfide source that is responsible for cell-associated β-$HgS_{(s)}$ formation when exogenous cysteine is not added to cells. Specifically, we tested the ISC and SUF systems whose role are to assemble Fe-S clusters in *E. coli*. Hg(II) displaces Fe(II) from Fe-S clusters *in vivo* in *E. coli* at micromolar Hg concentrations[57] and *in vitro* from the [4Fe-4S] cluster

of dehydratase family enzymes.[58] Thus, Fe-S clusters could be a source of sulfide for β-$HgS_{(s)}$ formation. Specifically, we exposed *iscS* and *sufS* mutants to 500 nM Hg(II) for 3 hours. IscS and SufS perform the same function of removing the S^0 from L-cysteine and donating it to the scaffold protein for Fe-S cluster formation, but the ISC system operates under normal conditions, while the SUF system functions under stress conditions.[19] From the HR-XANES spectra, the loss of the *sufS* gene had no effect on the Hg(II) coordination environment for cells exposed to 500 nM Hg(II) (Figure 5A and S3A). In contrast, the linear combination fit to the spectra of the *iscS* mutant exposed to 500 nM Hg(II) indicates less β-$HgS_{(s)}$ compared to the wild-type and *sufS* mutant. Therefore, Fe-S clusters are a likely sulfide source for β-$HgS_{(s)}$ formation under normal growth conditions, although more work should be done to determine the effect of *iscS* loss on cell physiology. The deletion of genes involved in cysteine degradation to sulfide for Fe-S cluster formation did not eliminate $HgS_{(s)}$ formation in cell samples, likely due to the fact that only single gene deletion mutants were tested. However, microbial cells are not viable after the elimination of both ISC and SUF mechanisms for Fe-S cluster formation without significantly altering cell metabolism.[59] In addition, another sulfide source in the cell that was not tested in this study could be assimilatory sulfate reduction, which is the primary route of cysteine synthesis in bacteria like *E. coli* and *Salmonella enterica* serovar Typhimurium.[27] In this pathway, which differs from dissimilatory sulfate reduction by anaerobic organisms,[60] sulfate is reduced to sulfite and then sulfide via sulfite reductase. Cysteine is then synthesized from sulfide and O-acetylserine with O-acetylserine (thiol)-lyase.

We found a striking difference in the HR-XANES spectra of the same sample (wild-type exposed to 50 nM Hg + 1 mM cysteine) that was prepared by 2 different methods for HR-XANES collection. The first method, which was used for all samples in this study, involved flash freezing the sample in liquid nitrogen and keeping it frozen throughout the measurement. The second method involved flash-freezing the sample in liquid nitrogen, freeze-drying, pressing into a pellet, and re-freezing prior to data collection (compare Figure 5D and Figure S3C). We observed a similar change in Hg speciation (with XAS analysis) after a flash-frozen sample thawed and then re-froze, although it was not freeze-dried.[36] The

freeze/thaw process may deteriorate the cell's membrane integrity, causing a change in Hg(II) speciation in the cell. Freeze-drying bacteria without a cryo-protectant (e.g., 10% sucrose) will compromise membrane integrity,[61] and implies that the cell-associated Hg species, at least for that particular sample, is sensitive to membrane damage. Fe-S clusters exist under reducing conditions in cells, are sensitive to oxygen species, and decompose upon exposure.[62] Hg-S clusters may have a similar sensitivity to oxygen exposure.

Implications for Hg(II) bioavailability

Early bacterial Hg(II) uptake studies suggested that neutral Hg(II)-sulfide complexes formed the bioavailable fraction of Hg(II) and were transported across the cell membrane layers by passive diffusion.[33, 63] More recently, evidence for energy-dependent Hg(II) biouptake has been reported, although these experiments were all performed in the presence of thiols (mainly cysteine). Schaefer et al. proposed that the entire Hg(II)-cysteine complex was taken up by an unknown metal-transport protein.[4] Liu et al. stated that cysteine may facilitate the ligand exchange of Hg(II) with a metal transport protein responsible for Hg(II) biouptake.[14]

We show herein that when *E. coli* is exposed to Hg(II)-cysteine complexes in the presence of excess cysteine, Hg(II) will become associated with the wild-type strain but not a cysteine desulfhydrase deletion mutant under otherwise the same experimental conditions and with minimal differences in cell physiology (as determined by cellular ATP concentration). The main difference between the wild-type and *decR* mutant assays involving added cysteine was the concentration of total sulfide in the exposure medium, and calculations for Hg(II)-sulfide species formation correlate with our measurements for cell-bound Hg(II). The degradation of cysteine to sulfide is an energy dependent process, which could have been mistakenly recognized as an active transport mechanism for Hg(II) biouptake in the presence of added cysteine in past studies. Thermodynamic calculations for $HgS_{(s)}$ formation are rather accurate in predicting when Hg(II) becomes associated with the cells, indicating that the ligand exchange from Hg(II)-cysteine complexes to Hg(II)-sulfides is not kinetically limited at the time scale of our experiment.

The Hg L_{III}-edge HR-XANES spectra never indicate that $Hg(SR)_2$ species are associated with either the wild-type or *decR* mutant cells after exposure to Hg(II) in the presence of excess cysteine; the cell-associated Hg(II) is either clearly $HgS_{(s)}$ or Hg-S clusters with a Hg coordination number greater than 3. This suggests that ligand exchange reactions between $Hg(SR)_2$ complexes outside the cell (i.e., $Hg(cysteine)_2$) and thiols in the cell membrane are not favorable. While our evidence suggests that the Hg(II) uptake pathway in the presence of excess cysteine involves a speciation change from Hg(II)-cysteine complexes to Hg(II)-sulfide species and Hg-S clusters, the uptake pathway remains unknown.

Understanding the formation of the cell-associated Hg-S clusters observed by HR-XANES both in the presence and absence of added excess cysteine could provide some insight into the Hg(II) uptake mechanism. Potentially, the Hg-S clusters are analogous to Fe-S clusters in proteins and capped by cysteine, which could create the HR-XANES spectra that we observe. As suggested by Manceau et al., it is also possible that Fe-S clusters serve as the scaffold for HgS nucleation, leading to the formation of a HgS mineral core that is functionalized by cysteine residues.[49] Depending on the total added Hg concentration, the seed HgS mineral may have only a few Hg atoms, and classify as a Hg-S cluster. There might also be a biological response from the ISC and SUF systems upon Hg exposure to sequester Hg(II) as HgS.[64] Although we only have evidence of Hg-S cluster formation after 3 hours of exposure and no localization information, it is possible that these Hg species that dominate the cell-associated Hg at the lowest tested Hg concentrations are the form that undergoes biouptake.

Because our results suggest that Hg(II)-sulfide species formation is a critical step for bacterial Hg(II) uptake in the presence of excess added cysteine, it is interesting that previous studies have shown that the presence of sulfide alone (in the absence of exogenous thiols) prevents Hg(II) uptake.[4, 65] This is likely due to the formation of $HgS_{(s)}$ particles that are too large to be bioavailable.[35] Graham et al. suggested that the coexistence of cysteine and sulfide can promote the formation of small, disordered $HgS_{(s)}$ nanoparticles that are able to passively diffuse through the cell's membrane layers.[10, 12] Our previous results with STEM-EDS provided direct evidence of $HgS_{(s)}$ nanoparticles attached to the cell

surface/extracellular matrix in *E. coli* and *G. sulfurreducens* that were likely physically limited from entering the cell cytoplasm.[35] Potentially, Hg(II)-sulfide complexes and/or small Hg-S clusters enter the cytoplasm via passive diffusion, as suggested previously, and the size of the Hg(II)-sulfide species is an important factor determining bioavailability.

Conclusion

The present study demonstrates that the bacterial sulfur metabolism (beyond dissimilatory sulfate reduction) can have a large influence on cell-associated Hg(II) coordination and Hg(II) biouptake. We show that the degradation of cysteine to sulfide and the formation of Hg(II)-sulfide species are critical for the biouptake of Hg(II) in the presence of excess cysteine in the exposure medium. These results may help elucidate Hg(II) bioavailability under sulfidic conditions where both sulfide and thiolate groups of organic matter compete to bind Hg(II) in environmental systems. Although these studies have been conducted with *E. coli*, which is unable to methylate Hg(II), many diverse organisms, in addition to *E. coli*, experience enhanced Hg(II) uptake with added cysteine, including Hg-methylators (e.g., *G. sulfurreducens*,[4, 5] *Desulfovibrio desulfuricans*,[4] *Geobacter bemidjiensis* Bem[15]) and other non-methylators (e.g., *Shewanella Oneidensis*[3]). Also, many diverse organisms are known to degrade cysteine by desulfhydrase enzymes.[27, 30, 66, 67] Therefore, the findings from this study on *E. coli* likely apply to organisms that are similarly affected by cysteine in their uptake of Hg(II). The role of cellular sulfur metabolism, and in particular Fe-S clusters, in relation to Hg(II) biouptake should be explored further.

Conflicts of Interest

There are no conflicts of interest to declare.

Acknowledgements

This work is supported by the National Science Foundation under grant CHE-1308504 and is based upon research supported by the Chateaubriand Fellowship of the Office for Science & Technology of the Embassy of France in the United States. We thank Dr. Mireille Chevallet and Dr. Xavier Maréchal for

assistance with the bacterial cultures. The experiments were performed on beamlines BM30B – FAME – and BM16 – UHD-FAME – at the European Synchrotron Radiation Facility (ESRF), Grenoble, France. The FAME-UHD project is financially supported by the French "grand emprunt" EquipEx (EcoX, ANR-10-EQPX-27-01), the CEA-CNRS CRG consortium and the INSU CNRS institute. We are grateful for the beamline assistance of Dr. Olivier Proux and Dr. Mauro Rovezzi at the ESRF. The TEM work made use of the BioCryo and EPIC facility of Northwestern University's NU*ANCE* Center, which has received support from the Soft and Hybrid Nanotechnology Experimental (SHyNE) Resource (NSF ECCS-1542205); the MRSEC program (NSF DMR-1121262) at the Materials Research Center; the International Institute for Nanotechnology (IIN); the Keck Foundation; and the State of Illinois, through the IIN. We thank Dr. Jinsong Wu for his assistance with the STEM and TEM imaging.

References

1. J. M. Parks, A. Johs, M. Podar, R. Bridou, R. A. Hurt, S. D. Smith, S. J. Tomanicek, Y. Qian, S. D. Brown, C. C. Brandt, A. V. Palumbo, J. C. Smith, J. D. Wall, D. A. Elias and L. Y. Liang, The genetic basis for bacterial mercury methylation, *Science*, 2013, **339**, 1332-1335.
2. S. A. Chiasson-Gould, J. M. Blais and A. J. Poulain, Dissolved organic matter kinetically controls mercury bioavailability to bacteria, *Environmental Science & Technology*, 2014, **48**, 3153-3161.
3. A. Szczuka, F. M. M. Morel and J. K. Schaefer, Effect of thiols, zinc, and redox conditions on hg uptake in shewanella oneidensis, *Environmental Science & Technology*, 2015, **49**, 7432-7438.
4. J. K. Schaefer, S. S. Rocks, W. Zheng, L. Y. Liang, B. H. Gu and F. M. M. Morel, Active transport, substrate specificity, and methylation of hg(ii) in anaerobic bacteria, *P Natl Acad Sci USA*, 2011, **108**, 8714-8719.
5. J. K. Schaefer and F. M. M. Morel, High methylation rates of mercury bound to cysteine by geobacter sulfurreducens, *Nat Geosci*, 2009, **2**, 123-126.
6. L. Zhao, H. Chen, X. Lu, H. Lin, G. A. Christensen, E. M. Pierce and B. Gu, Contrasting effects of dissolved organic matter on mercury methylation by geobacter sulfurreducens pca and desulfovibrio desulfuricans nd132, *Environmental Science & Technology*, 2017, **51**, 10468-10475.
7. H. Lin, X. Lu, L. Y. Liang and B. H. Gu, Cysteine inhibits mercury methylation by geobacter sulfurreducens pca mutant delta omcbestz, *Environ Sci Tech Let*, 2015, **2**, 144-148.

8. A. L. Dahl, J. Sanseverino and J. F. Gaillard, Bacterial bioreporter detects mercury in the presence of excess edta, *Environ Chem*, 2011, **8**, 552-560.

9. U. Ndu, T. Barkay, R. P. Mason, A. T. Schartup, R. Al-Farawati, J. Liu and J. R. Reinfelder, The use of a mercury biosensor to evaluate the bioavailability of mercury-thiol complexes and mechanisms of mercury uptake in bacteria, *Plos One*, 2015, **10**.

10. A. M. Graham, G. R. Aiken and C. C. Gilmour, Dissolved organic matter enhances microbial mercury methylation under sulfidic conditions, *Environmental Science & Technology*, 2012, **46**, 2715-2723.

11. S. A. Thomas, T. Z. Tong and J. F. Gaillard, Hg(ii) bacterial biouptake: The role of anthropogenic and biogenic ligands present in solution and spectroscopic evidence of ligand exchange reactions at the cell surface, *Metallomics*, 2014, **6**, 2213-2222.

12. A. M. Graham, G. R. Aiken and C. C. Gilmour, Effect of dissolved organic matter source and character on microbial hg methylation in hg-s-dom solutions, *Environmental Science & Technology*, 2013, **47**, 5746-5754.

13. U. Skyllberg, Competition among thiols and inorganic sulfides and polysulfides for hg and mehg in wetland soils and sediments under suboxic conditions: Illumination of controversies and implications for mehg net production, *J Geophys Res-Biogeo*, 2008, **113**.

14. Y. R. Liu, X. Lu, L. D. Zhao, J. An, J. Z. He, E. M. Pierce, A. Johs and B. H. Gu, Effects of cellular sorption on mercury bioavailability and methylmercury production by desulfovibrio desulfuricans nd132, *Environmental Science & Technology*, 2016, **50**, 13335-13341.

15. X. Lu, Y. R. Liu, A. Johs, L. D. Zhao, T. S. Wang, Z. M. Yang, H. Lin, D. A. Elias, E. M. Pierce, L. Y. Liang, T. Barkay and B. H. Gu, Anaerobic mercury methylation and demethylation by geobacter bemidjiensis bem, *Environmental Science & Technology*, 2016, **50**, 4366-4373.

16. A. Sekowska, H. F. Kung and A. Danchin, Sulfur metabolism in escherichia coli and related bacteria: Facts and fiction, *J Mol Microb Biotech*, 2000, **2**, 145-177.

17. N. M. Kredich, Biosynthesis of cysteine, *EcoSal Plus*, 2008, **3**.

18. D. C. Johnson, D. R. Dean, A. D. Smith and M. K. Johnson, Structure, function, and formation of biological iron-sulfur clusters, *Annu Rev Biochem*, 2005, **74**, 247-281.

19. B. Blanc, C. Gerez and S. A. de Choudens, Assembly of fe/s proteins in bacterial systems biochemistry of the bacterial isc system, *Bba-Mol Cell Res*, 2015, **1853**, 1436-1447.

20. Y. Bai, T. Chen, T. Happe, Y. Lu and A. Sawyer, Iron-sulphur cluster biogenesis via the suf pathway, *Metallomics*, 2018, **10**.

21. E. L. Mettert and P. J. Kiley, How is fe-s cluster formation regulated?, *Annual Review of Microbiology, Vol 69*, 2015, **69**, 505-526.

22. B. Roche, L. Aussel, B. Ezraty, P. Mandin, B. Py and F. Barras, Iron/sulfur proteins biogenesis in prokaryotes: Formation, regulation and diversity, *Bba-Bioenergetics*, 2013, **1827**, 455-469.

23. S. J. Lippard and J. M. Berg, *Principles of bioinorganic chemistry*, University Science Books, Mill Valley, CA, 1994.

24. E. Guédon and I. Martin-Verstraete, in *Amino acid biosynthesis ~ pathways, regulation and metabolic engineering*, ed. V. F. Wendisch, Springer Berlin Heidelberg, Berlin, Heidelberg, 2007, DOI: 10.1007/7171_2006_060, pp. 195-218.

25. N. Awano, M. Wada, H. Mori, S. Nakamori and H. Takagi, Identification and functional analysis of escherichia coli cysteine desulfhydrases, *Applied and Environmental Microbiology*, 2005, **71**, 4149-4152.

26. N. Awano, M. Wada, A. Kohdoh, T. Oikawa, H. Takagi and S. Nakamori, Effect of cysteine desulfhydrase gene disruption on l-cysteine overproduction in escherichia coli, *Appl Microbiol Biot*, 2003, **62**, 239-243.

27. T. Oguri, B. Schneider and L. Reitzer, Cysteine catabolism and cysteine desulfhydrase (cdsh/stm0458) in salmonella enterica serovar typhimurium, *J Bacteriol*, 2012, **194**, 4366-4376.

28. T. Shimada, K. Tanaka and A. Ishihama, Transcription factor decr (ybao) controls detoxification of l-cysteine in escherichia coli, *Microbiol-Sgm*, 2016, **162**, 1698-1707.

29. S. I. Tchong, H. M. Xu and R. H. White, L-cysteine desulfidase: An [4fe-4s] enzyme isolated from methanocaldococcus jannaschii that catalyzes the breakdown of l-cysteine into pyruvate, ammonia, and sulfide, *Biochemistry-Us*, 2005, **44**, 1659-1670.

30. K. Takumi and G. Nonaka, Bacterial cysteine-inducible cysteine resistance systems, *J Bacteriol*, 2016, **198**, 1384-1392.

31. A. K. Bachhawat and A. Kaur, Glutathione degradation, *Antioxid Redox Sign*, 2017, **27**, 1200-1216.

32. H. Suzuki, S. Kamatani, E.-S. Kim and H. Kumagai, Aminopeptidases a, b, and n and dipeptidase d are the four cysteinylglycinases of escherichia colik-12, *J Bacteriol*, 2001, **183**, 1489.

33. J. M. Benoit, C. C. Gilmour and R. P. Mason, Aspects of bioavailability of mercury for methylation in pure cultures of desulfobulbus propionicus (1pr3), *Applied and Environmental Microbiology*, 2001, **67**, 51-58.

34. A. Drott, L. Lambertsson, E. Björn and U. Skyllberg, Importance of dissolved neutral mercury sulfides for methyl mercury production in contaminated sediments, *Environmental Science & Technology*, 2007, **41**, 2270-2276.

35. S. A. Thomas, K. E. Rodby, E. W. Roth, J. Wu and J.-F. Gaillard, Spectroscopic and microscopic evidence of biomediated hgs species formation from hg(ii)–cysteine complexes: Implications for hg(ii) bioavailability, *Environmental Science & Technology*, 2018, **52**, 10030-10039.

36. S. A. Thomas and J.-F. Gaillard, Cysteine addition promotes sulfide production and 4-fold hg(ii)–s coordination in actively metabolizing escherichia coli, *Environmental Science & Technology*, 2017, **51**, 4642-4651.

37. T. Baba, T. Ara, M. Hasegawa, Y. Takai, Y. Okumura, M. Baba, K. A. Datsenko, M. Tomita, B. L. Wanner and H. Mori, Construction of escherichia coli k-12 in-frame, single-gene knockout mutants: The keio collection, *Mol Syst Biol*, 2006, **2**.

38. C. Ranquet, S. Ollagnier-de-Choudens, L. Loiseau, F. Barras and M. Fontecave, Cobalt stress in escherichia coli - the effect on the iron-sulfur proteins, *J Biol Chem*, 2007, **282**, 30442-30451.

39. J. D. Cline, Spectrophotometric determination of hydrogen sulfide in natural waters, *Limnol Oceanogr*, 1969, **14**, 454-&.

40. P. Nagy, Z. Palinkas, A. Nagy, B. Budai, I. Toth and A. Vasas, Chemical aspects of hydrogen sulfide measurements in physiological samples, *Bba-Gen Subjects*, 2014, **1840**, 876-891.

41. M. K. Gaitonde, A spectrophotometric method for direct determination of cysteine in presence of other naturally occurring amino acids, *Biochem J*, 1967, **104**, 627-&.

42. B. Mishra, E. J. O'Loughlin, M. I. Boyanov and K. M. Kemner, Binding of hg-ii to high-affinity sites on bacteria inhibits reduction to hg-0 by mixed fe-ii/iii phases, *Environmental Science & Technology*, 2011, **45**, 9597-9603.

43. O. Proux, E. Lahera, W. Del Net, I. Kieffer, M. Rovezzi, D. Testemale, M. Irar, S. Thomas, A. Aguilar-Tapia, E. F. Bazarkina, A. Prat, M. Tella, M. Auffan, J. Rose and J.-L. Hazemann, High-energy resolution fluorescence detected x-ray absorption spectroscopy: A powerful new structural tool in environmental biogeochemistry sciences, *Journal of Environmental Quality*, 2017, DOI: 10.2134/jeq2017.01.0023.

44. B. Ravel and M. Newville, Athena, artemis, hephaestus: Data analysis for x-ray absorption spectroscopy using ifeffit, *J Synchrotron Radiat*, 2005, **12**, 537-541.

45. http://www.eawag.ch/en/department/surf/projects/chemeql/ (accessed Nov. 12, 2016).

46. G. Nonaka and K. Takumi, Cysteine degradation gene yham, encoding cysteine desulfidase, serves as a genetic engineering target to improve cysteine production in escherichia coli, *Amb Express*, 2017, **7**.

47. H. Y. Hu, H. Lin, W. Zheng, B. Rao, X. B. Feng, L. Y. Liang, D. A. Elias and B. H. Gu, Mercury reduction and cell-surface adsorption by geobacter sulfurreducens pca, *Environmental Science & Technology*, 2013, **47**, 10922-10930.

48. S. P. M. Crouch, R. Kozlowski, K. J. Slater and J. Fletcher, The use of atp bioluminescence as a measure of cell-proliferation and cytotoxicity, *J Immunol Methods*, 1993, **160**, 81-88.

49. A. Manceau, J. X. Wang, M. Rovezzi, P. Glatzel and X. B. Feng, Biogenesis of mercury-sulfur nanoparticles in plant leaves from atmospheric gaseous mercury, *Environmental Science & Technology*, 2018, **52**, 3935-3948.

50. A. Manceau, M. Enescu, A. Simionovici, M. Lanson, M. Gonzalez-Rey, M. Rovezzi, R. Tucoulou, P. Glatzel, K. L. Nagy and J. P. Bourdineaud, Chemical forms of mercury in human hair reveal sources of exposure, *Environmental Science & Technology*, 2016, **50**, 10721-10729.

51. A. Manceau, C. Lemouchi, M. Enescu, A. C. Gaillot, M. Lanson, V. Magnin, P. Glatzel, B. A. Poulin, J. N. Ryan, G. R. Aiken, I. Gautier-Luneau and K. L. Nagy, Formation of mercury sulfide from hg(ii)-thiolate complexes in natural organic matter, *Environmental Science & Technology*, 2015, **49**, 9787-9796.

52. A. Manceau, M. Merkulova, M. Murdzek, V. Batanova, R. Baran, P. Glatzel, B. K. Saikia, D. Paktunc and L. Lefticariu, Chemical forms of mercury in pyrite: Implications for predicting

mercury releases in acid mine drainage settings, *Environmental Science & Technology*, 2018, DOI: 10.1021/acs.est.8b02027.

53. R. A. Steele and S. J. Opella, Structures of the reduced and mercury-bound forms of merp, the periplasmic protein from the bacterial mercury detoxification system, *Biochemistry-Us*, 1997, **36**, 6885-6895.

54. A. Deonarine and H. Hsu-Kim, Precipitation of mercuric sulfide nanoparticles in nom-containing water: Implications for the natural environment, *Environmental Science & Technology*, 2009, **43**, 2368-2373.

55. A. Manceau, C. Lemouchi, M. Rovezzi, M. Lanson, P. Gatzel, K. L. Nagy, I. Gautier-Luneau, Y. Joly and M. Enescu, Structure, bonding, and stability of mercury complexes with thiolate and thioether ligands from high-resolution xanes spectroscopy and first-principles calculations, *Inorganic Chemistry*, 2015, **54**, 11776-11791.

56. J.-P. Bourdineaud, M. Gonzalez-Rey, M. Rovezzi, P. Glatzel, K. L. Nagy and A. Manceau, Divalent mercury in dissolved organic matter is bioavailable to fish and accumulates as dithiolate and tetrathiolate complexes, *Environmental Science & Technology*, 2019, DOI: 10.1021/acs.est.8b06579.

57. S. P. LaVoie, D. T. Mapolelo, D. M. Cowart, B. J. Polacco, M. K. Johnson, R. A. Scott, S. M. Miller and A. O. Summers, Organic and inorganic mercurials have distinct effects on cellular thiols, metal homeostasis, and fe-binding proteins in escherichia coli, *JBIC Journal of Biological Inorganic Chemistry*, 2015, **20**, 1239-1251.

58. F. F. Xu and J. A. Imlay, Silver(i), mercury(ii), cadmium(ii), and zinc(ii) target exposed enzymic iron-sulfur clusters when they toxify escherichia coli, *Applied and Environmental Microbiology*, 2012, **78**, 3614-3621.

59. N. Tanaka, M. Kanazawa, K. Tonosaki, N. Yokoyama, T. Kuzuyama and Y. Takahashi, Novel features of the isc machinery revealed by characterization of escherichia coli mutants that survive without iron–sulfur clusters, *Mol Microbiol*, 2015, **99**, 835-848.

60. N. Pfennig, F. Widdel and H. G. Trüper, in *The prokaryotes: A handbook on habitats, isolation, and identification of bacteria*, eds. M. P. Starr, H. Stolp, H. G. Trüper, A. Balows and H. G. Schlegel, Springer Berlin Heidelberg, Berlin, Heidelberg, 1981, DOI: 10.1007/978-3-662-13187-9_74, pp. 926-940.

61. P. Wessman, S. Hakansson, K. Leifer and S. Rubino, Formulations for freeze-drying of bacteria and their influence on cell survival, *Jove-J Vis Exp*, 2013, DOI: UNSP e4058

10.3791/4058.

62. J. A. Imlay, Iron-sulphur clusters and the problem with oxygen, *Mol Microbiol*, 2006, **59**, 1073-1082.

63. J. M. Benoit, C. C. Gilmour, R. P. Mason and A. Heyes, Sulfide controls on mercury speciation and bioavailability to methylating bacteria in sediment pore waters, *Environmental Science & Technology*, 1999, **33**, 951–957.

64. S. P. LaVoie and A. O. Summers, Transcriptional responses of escherichia coli during recovery from inorganic or organic mercury exposure, *BMC Genomics*, 2018, **19**, 52.

65. T. Zhang, B. Kim, C. Leyard, B. C. Reinsch, G. V. Lowry, M. A. Deshusses and H. Hsu-Kim, Methylation of mercury by bacteria exposed to dissolved, nanoparticulate, and microparticulate mercuric sulfides, *Environmental Science & Technology*, 2012, **46**, 6950-6958.

66. C. W. Forsberg, Sulfide production from cysteine by desulfovibrio-desulfuricans, *Applied and Environmental Microbiology*, 1980, **39**, 453-455.

67. A. M. Graham, A. L. Bullock, A. C. Maizel, D. A. Elias and C. C. Gilmour, Detailed assessment of the kinetics of hg-cell association, hg methylation, and methylmercury degradation in several desulfovibrio species, *Applied and Environmental Microbiology*, 2012, **78**, 7337-7346.

Figures

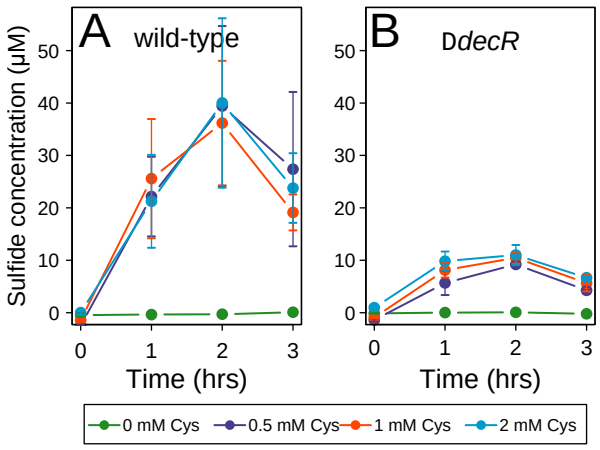

Figure 1: The concentration of sulfide in the exposure medium detected after 3-hour exposures of (A) wild-type and (B) *decR* mutant strains of *E. coli* to 0, 0.5, 1, and 2 mM cysteine (Cys). The points are averages from 3 independent experiments and the error bars are ± 1 S.D.

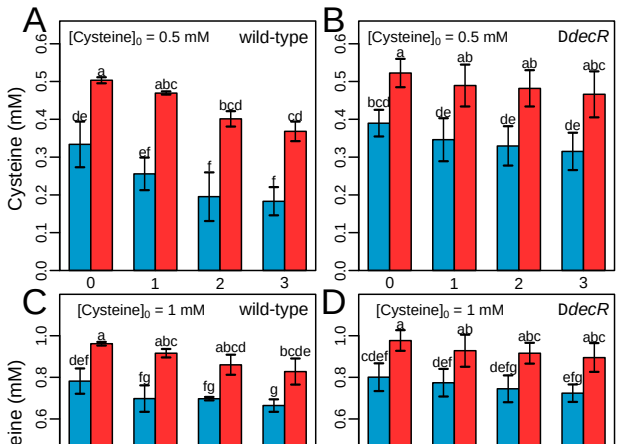
A
[Cysteine]0 = 0.5 mM
wild-type
B
[Cysteine]0 = 0.5 mM
DdecR
C
[Cysteine]0 = 1 mM
wild-type
D
[Cysteine]0 = 1 mM
DdecR
Cysteine (mM)
0
1
2
3

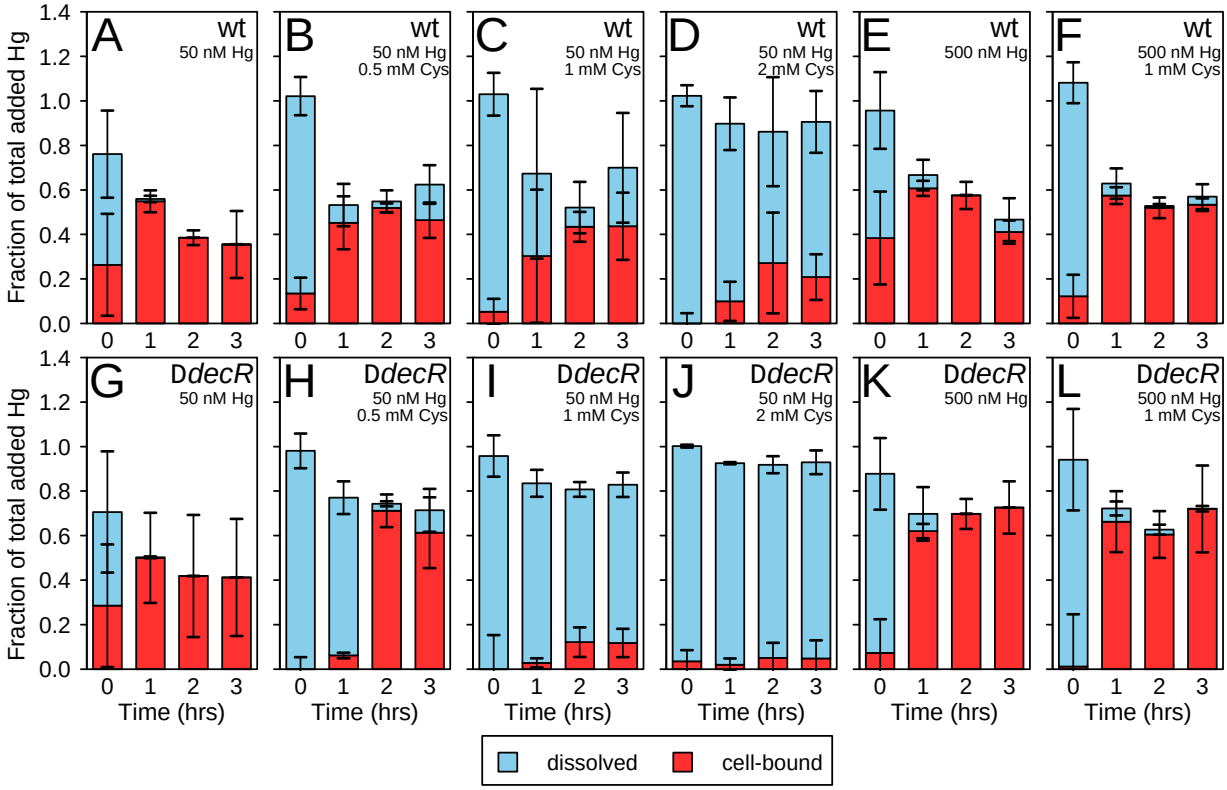

Figure 3: The dissolved and cell-bound Hg presented as a fraction of the total added Hg (i.e., 50 or 500 nM) detected after 0 to 3 hours of exposure of the (A - F) wild-type (wt) and (G - L) *decR* mutant to 50 or 500 nM total Hg. The added Hg was pre-equilibrated with either (A, E, G, K) 0 mM cysteine (Cys), (B, H) 0.5 mM Cys, (C, F, I, L) 1 mM Cys, or (D, J) 2 mM Cys. In many cases, the sum of the dissolved and cell-bound bars does not add to the total added Hg likely due to loss from Hg(II) reduction to Hg(0) and volatilization. The bars are averages from 2-3 independent experiments and the error bars are ± 1 S.D.

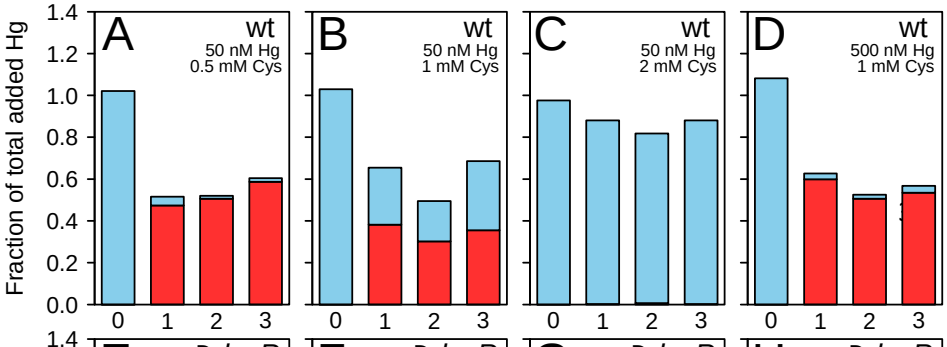
Fraction of total added Hg
1.4
1.2
1.0
0.8
0.6
0.4
0.2
0.0
A
wt
50 nM Hg
0.5 mM Cys
B
wt
50 nM Hg
1 mM Cys
C
wt
50 nM Hg
2 mM Cys
D
wt
500 nM Hg
1 mM Cys
0
1
2
3

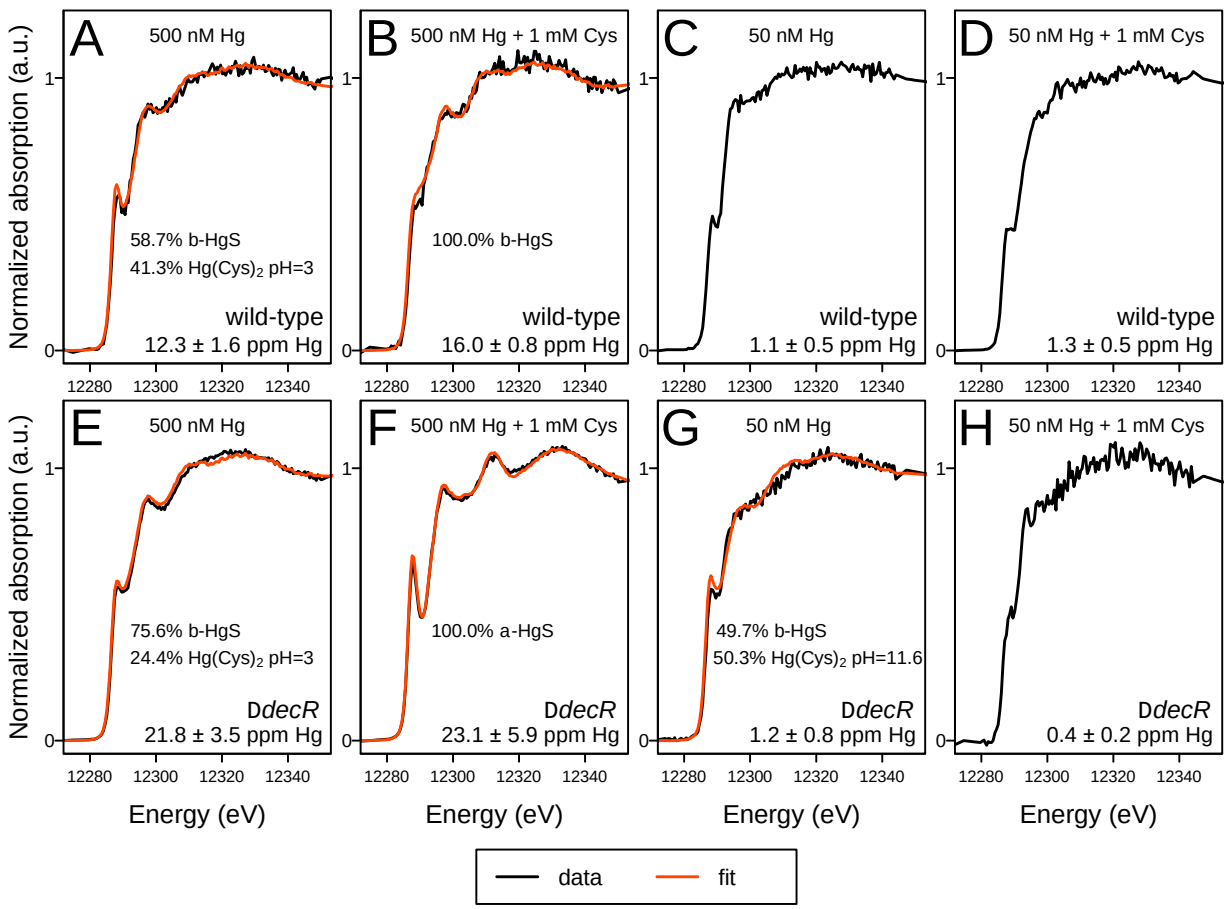

Figure 5: Hg L_{III}-edge HR-XANES of cell pellets of (A,B,C,D) wild-type and (E,F,G,H) *decR* mutant strains of *E. coli* that were initially exposed to 50 and 500 nM Hg with and without cysteine for 3 hours. The red line is the best-fit result of a linear combination fit, which included β-HgS, α-HgS, $Hg(Cys)_{2(aq)}$ at pH=3, and $Hg(Cys)_{2(aq)}$ at pH=11.6 as references. The spectra in plots C, D, and H are missing a best-fit result due to the absence of a reference spectrum that fits well; however, the spectra in plots C, D, and H do not contain prominent in-edge peaks that signify Hg coordination to 2 sulfur atoms. The concentration of cell-associated Hg (ppm) for each spectrum is included at the bottom of each plot.